PHYSICAL REVIEW B VOLUME 16, NUMBER 12 15 DECEMBER 1977

High-dose neutron-irradiation effects in fcc metals at 4.6 K*

M. Nakagawa,† K. Böning, P. Rosner, and G. Vogl
Physik-Department, Technische Universität München, D-8046 Garching, Germany
(Received May 16, 1977)

The rate of residual-resistivity increase and the isochronal recovery have been studied on the fcc metals Al, Ni, Cu, Pd, Ag, Pt, and Au irradiated at 4.6 K with reactor neutrons to a dose of about 10^{19} fast neutrons/cm^2. The rate of resistivity increase is nonlinear as a function of irradiation-induced resistivity; computer analysis shows that the data are best fitted with an expression having up to third-order terms in $\Delta\rho$. There are deviations from simple damage-rate theory in all cases, but an anomalous negative deviation from a linear law (convex curvature) is observed in Ni, Pd, Pt (and Fe). This behavior is most probably caused by a decrease of the specific Frenkel-defect resistivity due to defect clustering, an effect which should contribute in all metals after fast-neutron irradiation to high doses. Saturation values of resistivity and defect concentration as well as recombination volumes have been obtained more accurately than from previous work. The isochronal recovery is compared with previous lower-dose data. Stage I decreases and stage III increases with increasing neutron dose. After high-dose irradiation, correlated recovery in stage III becomes dominant in the case of Al, Cu, Ag, and Au.

I. INTRODUCTION

Irradiation of metals with high-energy particles produces Frenkel defects (FD), i.e., self-interstitials and vacancies, which are stable only at very low temperature.[1] With increasing irradiation dose the FD concentration c generally approaches some saturation value c_s (typically several 10^{-3}), since newly produced FD will more and more recombine immediately with already existing FD. This "radiation annealing" effect is very complicated microscopically, since at high doses same-type defects (e.g., interstitials) have an increasing tendency to form clusters, i.e., their spontaneous recombination volumes v_0 overlap leading to smaller "effective" recombination volumes and a higher possible value of c_s.[2-6] In experimental "dose curves" at 4 K usually the increase $\Delta\rho$ of the residual resistivity ρ is measured and assumed to be proportional to c. For an understanding of radiation damage it is important to know these experimental curves up to high irradiation doses, as well as their differences for various metals or different types of bombarding particles. Warming up the samples isochronically after irradiation, the observed recovery behavior of c (respective of $\Delta\rho$) is also affected by these specific details of the initial FD concentration and configuration.[7,8]

Within reasonably short irradiation time (say ten days or less), the FD saturation concentration c_s (respective of $\Delta\rho_s$) can be practically reached only in special cases. Radiation damage by fission fragments has been investigated in 4-K reactor irradiations of natural uranium (see, e.g., Ref. 9) or[10] of Cu-doped with ^{235}U; here the experimental $\Delta\rho_{max}$ came up to about 99% of the extrapolated $\Delta\rho_s$. Heavy-ion irradiations of thin foils allow similar high-damage values.[11] Electron irradiation at 4 K produces essentially isolated interstitials and vacancies and so is especially suited for comparison with theoretical models; here ratios $\Delta\rho_{max}/\Delta\rho_s$ of up to 53%–79% have been obtained for various metals.[12] On the other hand, irradiation by reactor neutrons produces more or less dense cascades of FD[7,8,13] and is much more closely related to technical applications; here the largest values of $\Delta\rho_{max}/\Delta\rho_s$ achieved so far were about 43%–60% and 12%–40% in Refs. 14 and 15, respectively.

In this paper we report on new high-dose reactor irradiation experiments of various fcc metals at 4.6 K up to values of $\Delta\rho_{max}/\Delta\rho_s = 50\%-93\%$, and on subsequent isochronal annealing measurements. The special features of the present investigation are: (i) irradiation up to a dose $\phi t_{max} = 1.0\times10^{19}$ cm^{-2} of fast neutrons ($E>0.1$ MeV) which has never been reached before at 4.6 K; (ii) two simultaneous irradiations of eight samples each, allowing very precise checks and comparison of the individual results; (iii) very high measuring accuracy by use of an automatic measuring system and on-line computer; and (iv) least-squares fits of the results to theoretical laws of radiation damage in order to check these laws and obtain high-precision values for the underlying parameters. In some cases a striking anomalous behavior of the damage rate was obtained, which could not be resolved in (but is consistent with) the previous low-dose investigations. Finally, our results of the isochronal recovery after this high-dose reactor irradiation are compared with previous low-dose results.

II. EXPERIMENTAL

Two irradiation experiments have been performed with individual sample holders as shown in Fig. 1. Each sample holder was fastened to the end of a stainless-steel capillary (length 13 m) supporting all the electrical leads and two copper-constantan thermocouples. The polycrystalline sample wires (length 31 cm) were threaded through the Al_2O_3 capillaries (length 5 cm) having six holes each. Always eight samples were contained in one sample holder, arranged symmetrically about the sample-holder axis in the sequence as listed in Table I. The values of $\rho_0 = \rho_{4.6K}$ have been determined from the final RRR's using tabulated values[16] of ρ_{297K}. All relevant sample details are also collected in Table I and explained in the caption. All residual resistivity values given in this paper are without any size-effect corrections.

Electrically, all samples in a sample holder were connected in series and a current of 0.5 A was applied (short-term stability better than 10^{-5}). Current and potential leads were soldered directly

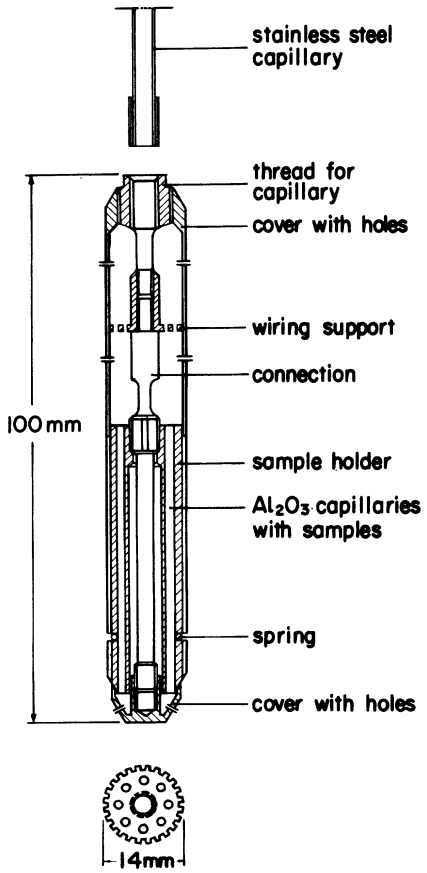

FIG. 1. Anodized Al sample holder as used for the irradiation experiments.

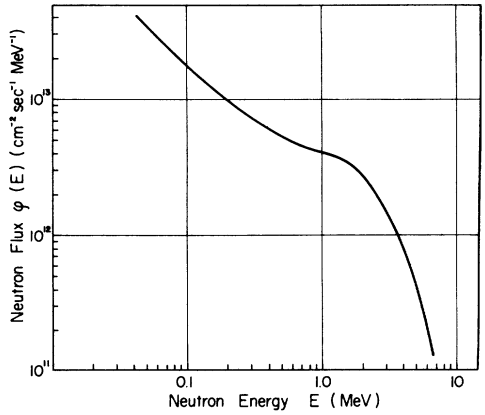

FIG. 2. The fast-neutron flux spectrum $\varphi(E) = d\phi/dE$ in the position of the low-temperature irradiation facility (Ref. 18).

to the samples, and the voltage drops on the samples and on a 10^{-2} Ω normal resistor as well as the thermocouple voltages were measured continuously with an automatic measuring system. This system involved a high-precision integrating digital voltmeter (resolution 100 nV) and a low-emf automatic input switch. A high rejection of thermal and other noise was achieved by integrating each voltage signal for 6 sec for both current directions. Finally, all data were fed into an on-line computer and the results stored on magnetic tape.

Both irradiations were performed at 4.6 K in the liquid-helium irradiation facility of the Munich Research Reactor (Forschungs Reaktor München).[17] During these irradiations all measurements were made *in situ* and the sample-holder position was never changed. The fast-neutron spectrum $\varphi(E) = d\phi/dE$ in the irradiation position was measured between both irradiation runs[18] and is shown in Fig. 2. The nominal value of the local-fast-neutron flux ϕ ($E > 0.1$ MeV) was $\phi_0 = 1.2 \times 10^{13}$ cm^{-2} sec^{-1}; the corresponding resonance flux (related to the gold resonance) was 1.2×10^{12} cm^{-2} sec^{-1}, and the thermal flux was 1.5×10^{13} cm^{-2} sec^{-1}. However, possible fluctuations or drifts of ϕ_0 with time were largely eliminated by use of a continuous local-fast-neutron flux monitor supplying a high-precision signal proportional to $\int \phi_0 dt$ as measured in about 2 cm distance from the cold sample[19] [flowing water is activated by the fast-neutron reaction $^{16}O(n,p)^{16}N$, and the resulting activity is counted; relative precision is about 10^{-3} during 10 days]. This value of the fast-flux ϕ_0 was assumed to be roughly identical with the value of the local-flux ϕ in the middle of the sample holder. However, to allow a reasonable comparison of the dose-curve results of the individual samples, it was necessary to

TABLE I. Sample specifications. The polycrystalline sample wires (diameter D) have been purchased from the indicated companies (99.999+%, e.g., means a nominal sample purity of better than 99.9995%). The residual-resistivity ratios (RRR), $\rho_{297K}/\rho_{4.6K}$, are given before and after the annealing treatment. The values of $\rho_0 = \rho_{4.6K}$ have been determined (always without any size-effect correction) from the final RRR's using tabulated values (Ref. 16) of ρ_{297K}. Finally, $\Delta\rho_{max}$ is the as-measured increase of the residual resistivity at the end of the irradiation, and the ϕt_{max} are the corresponding local fast-neutron doses (for $E > 0.1$ MeV).

Samples No.	Company	D (mm)	RRR	Preirradiation annealing	RRR	ρ_{297K} (nΩcm)	ρ_0 (nΩcm)	$\Delta\rho_{max}$ (nΩcm)	ϕt_{max} (10^{18} n/cm^2)
				(a) RUN I (Sample holder 1)					
Al(1)	MRC 99.999+%	0.245	275	500 °C, in air, 3 h	1351	2772	2.052	866.7	8.83
Ag(1)	Degussa 99.999%	0.18	116	700 °C, 3×10^{-2} Torr, 36 h	865	1612	1.864	361.0	8.73
Cu(1)	S. Cohn 99.999%	0.17	432	700 °C, 5×10^{-4} Torr, 2 h	1490	1757	1.179	321.4	8.49
Fe	Johnson-M.	0.20	16	800 °C, 2×10^{-5} Torr, 2 h	76	10298	135.5	4208.2	8.25
Al(2)	MRC 99.999+%	0.245	275	500 °C, in air, 3 h	1493	2729	1.828	847.4	8.15
Ni	MRC 99.99%	0.25	55	1000 °C, 8×10^{-3} Torr, 2 h	843	7293	8.651	1065.9	8.25
Cu(2)	S. Cohn 99.999%	0.16	432	700 °C, 5×10^{-4} Torr, 2 h	1464	1760	1.202	321.9	8.49
Pt(1)	S. Cohn 99.999%	0.10	97	1650 °C, in air, 30 min	2495	10584	4.242	1168.9	8.73
				(b) RUN II (Sample holder 2)					
Al(3)	MRC 99.999+%	0.245	275	500 °C, in air, 3 h	1470	2693	1.832	884.7	10.40
Pd	MRC 99.99%	0.25	7	1300 °C, 4×10^{-5} Torr, 10 min	301	10610	35.25	1096.7	10.46
Ag(2)	Degussa 99.999%	0.20	116	700 °C, 3×10^{-2} Torr, 36 h	1211	1646	1.359	408.1	10.40
Au	S. Cohn 99.999%	0.08	400	950 °C, in air, 10 h	809	2217	2.741	498.9	10.25
Al(4)	MRC 99.999+%	0.245	275	500 °C, in air, 3 h	1476	2692	1.824	881.6	10.09
Pt(2)	S. Cohn 99.999%	0.10	97	1650 °C, in air, 15 min	2022	10454	5.170	1265.1	10.03
Ag(3)	Degussa 99.999%	0.20	116	700 °C, 3×10^{-2} Torr, 36 h	1112	1561	1.404	393.4	10.09
Sn	E.S.P.I.	0.20	...	... ...	8090	10994	1.359	491.8	10.25

correct for a small linear gradient of ϕ over the sample holder (being independent of time). For this end, each sample holder contained two pairs of virtually identical samples arranged opposite to each other (see Table I and Fig. 1), and from the observed differences in $d\Delta\rho/d\phi_0 t$ for equal values of $\Delta\rho$, the vector $\vec{\nabla}\phi/\phi$ could be easily determined. From the corrected, local values of ϕt_{max} at the end of the irradiation as given in Table I (the $\Delta\rho_{max}$ are the corresponding resistivity increments), one can see that this effect is always smaller than about ±4% over the sample holder. During irradiation the computer stores all corresponding values of $\Delta\rho$ and $\phi_0 t$ (we always abbreviate $\phi t \equiv \int \phi dt$), so that we immediately know the results, $d\Delta\rho/d\phi_0 t$. After irradiation the local correction factors ϕ/ϕ_0 are determined, and from the stored data the computer calcu'ates the results, $\Delta\rho(\phi t)$ and $d\Delta\rho/d\phi t$. Finally, these data can be corrected for a possible resistivity contribution of radioisotopes and be least-squares fitted to various laws of radiation damage.

After irradiation the samples were pulled up into an annealing cryostat which was fixed on top of the irradiation loop.[6,17] Unfortunately, due to a defect on the refrigerator sample holder 1 warmed up till about 80 K during this procedure, but also sample holder 2 got warm till about 20 K (a second failure occured here in the annealing range 32–43 K). Nevertheless, due to the considerable expenditure involved in such high-dose experiments, we have continued with the full annealing program. The temperatures T have been measured with the sample copper-constantan thermocouples which as far as one knows are practically unaffected by the irradiation (compare Ref. 20). The isochronal anneals lasted 10 min each, and T was kept constant to about ±0.1 K.

III. DOSE-CURVE RESULTS AND DISCUSSION

A. Theoretical description of damage rate

In this paper we will always use the relation $\Delta\rho = \rho_F c$ where the Frenkel-defect specific resistivity ρ_F is assumed to be a constant in every metal. This relation should be rather well fulfilled during irradiation at least for not-too-high FD concentrations c (i.e., for single FD or relatively small FD clusters[13]), but could be distinctly violated during annealing when interstitial loops are being formed after stage I.[21–23]

For the mathematical description of defect production we follow the simple analytical treatment developed for electron irradiation, where essentially single vacancies and single interstitials are produced.[1,5] The further complications arising

in fast-neutron irradiations, where some FD clustering is possible already within a single-displacement cascade,[13] are difficult to be treated theoretically[5] and are not explicitly considered here.

Without any overlap of recombination volumes v_0 the damage rate would decrease due to radiation annealing as Ref. 1,

$$\frac{d\Delta\rho}{d\phi t} = \sigma_d \rho_F \left(1 - 2\frac{v_0 \Delta\rho}{\rho_F}\right), \tag{1}$$

where σ_d is some effective-displacement cross section (as discussed for the case of neutron irradiation in Ref. 24). For single overlap of recombination volumes,[1] a term $+v_0^2\Delta\rho^2/\rho_F^2$ must be added in the parenthesis of Eq. (1), and for higher-order overlap,[5] the next term in a series expansion is $-v_0^3\Delta\rho^3/(100\rho_F^3)$. It is further necessary to consider subthreshold energy transfers (cross section σ_s) which in the simplest case lead to a contribution $-g\sigma_s\Delta\rho/(\sigma_d\rho_F)$ in Eq. (1), with g being some geometrical factor.[1] So we finally arrive at the equation

$$\frac{d\Delta\rho}{d\phi t} = \sigma_d\rho_F - (2v_0\sigma_d + g\sigma_s)\Delta\rho + (v_0^2\sigma_d/\rho_F)\Delta\rho^2 - 0.01(v_0^3\sigma_d/\rho_F^2)\Delta\rho^3 . \tag{2}$$

For a check of this relation we have fitted our experimental results in most cases to the equation

$$\frac{d\Delta\rho}{d\phi t} = A + B\Delta\rho + C\Delta\rho^2 + D\Delta\rho^3 , \tag{3}$$

and a comparison of the shape of both curves (i.e., eliminating ϕt and essentially also σ_d) leads to the equations

$$D/A = -0.01 v_0^3/\rho_F^3 , \tag{4}$$

$$C/A = v_0^2/\rho_F^2 , \tag{5}$$

$$B/A = -2v_0/\rho_F - g\sigma_s/(\sigma_d\rho_F) , \tag{6}$$

from which v_0 and $g\sigma_s/\sigma_d\rho_F$ can be obtained;[25] ρ_F is assumed to be known. In Eqs. (4) and (5), v_0 is overdetermined and so the condition

$$100(D/A)(C/A)^{-3/2} = -1 \tag{7}$$

must be fulfilled, which represents a test to the validity of our analytical description of the experimental data (cubic test). Normally, v_0 was determined from Eq. (5). However, we also found cases where Eqs. (2) and (3) were basically violated because of $C/A < 0$ (convex curvature) or also $D/A > 0$. In these "exotic" cases, a very rough value of v_0 was estimated from the extrapolated saturation resistivity $\Delta\rho_s$ (where $d\Delta\rho/d\phi t = 0$),

$$v_0 = \rho_F/\Delta\rho_s , \tag{8}$$

as would follow from Eq. (2) neglecting subthreshold effects ($g\sigma_s = 0$) and the cubic term. In "normal" cases, the values v_0 following from Eqs. (5) and (8) can be compared to qualitatively illustrate the effect of subthreshold recombinations. More exactly, from Eqs. (2)–(6) one sees that in the linear region of the damage-rate decrease a fraction x of recombinations is due to subthreshold energy transfers (which push an otherwise stable interstitial into the recombination volume of a nearby vacancy, or vice versa)

$$x = \frac{g\sigma_s}{2v_0\sigma_d + g\sigma_s} = \frac{2(C/A)^{1/2} + B/A}{B/A} . \tag{9}$$

Only the rest $1 - x$ corresponds to spontaneous recombinations (where an interstitial is produced directly within the recombination volume of an already existing vacancy, or vice versa).

B. Experimental dose-curve results and fits

Our experimental results for the increase $\Delta\rho = \Delta\rho_{\text{exp}}$ of residual resistivity versus local fast-neutron dose ϕt are shown in Fig. 3 and Figs. 5–10, always for one sample of every metal since equivalent curves exactly fall upon each other. In the same figures we also show the differentiated dose curves $d\Delta\rho/d\phi t$ vs $\Delta\rho$ for all samples. The agreement of these curves $d\Delta\rho/d\phi t$ with computer fits is demonstrated in Fig. 4 for Al up to various orders of Eq. (3), and in Figs. 5–10 for the other metals with respect to the cubic Eq. (3) only (more explanation follows below). Not shown are the results for the non-fcc metals Fe[26] and Sn.[27]

In all figures and tables of this work ϕt means the fast-neutron dose, disregarding the fact that thermal and resonance neutrons contribute to the defect production too. The relative contribution of the thermal-neutron flux (Sec. II) to the initial damage production rate $d\Delta\rho/d\phi t$ can be estimated using the data of Ref. 28; the results are <0.5% for Al, 4.4% for Ni, 2.5% for Cu, 2.1% for Pd, 10.3% for Ag, 3.1% for Pt, and 10.7% for Au. Thus, this contribution is significant, especially in the cases of Ag and Au. The contribution of the resonance flux (Sec. II) to the initial damage production rate is non-negligible only in the cases of Ag and Au. In the case of Au it is estimated to be about one-quarter to one-third of the contribution from the thermal flux; in the case of Ag it should even be less.

During reactor irradiation, transmutations are induced in the samples which can also give a contribution to the measured resistivity increases $\Delta\rho = \Delta\rho_{\text{exp}}$. A survey is given in Table II, where the maximum concentrations $c_{\text{max}}^{\text{FA}}$ of produced foreign atoms (FA) are calculated for the thermal, resonance, and fast-neutron-flux values of Sec. II. The corresponding maximum resistivity contribu-

TABLE II. Influence of irradiation-induced transmutations on the dose curves. c_{max}^{FA} is the maximum concentration of foreign atoms (FA) at the end of the irradiation (fast-neutron dose ϕt_{max}) and the $\Delta\rho_{max}^{FA}$ are the corresponding resistivity contributions. The last two columns show which fractions of the experimental $\Delta\rho$, respectively, $d\Delta\rho/d\phi t$ (both taken at ϕt_{max}) are due to the FA. Transmutation corrections follow to be essential only for Ag and Au.

Samples	ϕt_{max} (10^{18} n/cm^2) thermal	ϕt_{max} (10^{17} n/cm^2) resonance	ϕt_{max} (10^{18} n/cm^2) fast	Transmutation elements FA	c_{max}^{FA} (ppm)	$\Delta\rho_{max}^{FA}$ (nΩ cm)	$\frac{\Delta\rho_{max}^{FA}}{\Delta\rho_{max}}$	$\left(\frac{d\Delta\rho^{FA}/d\phi t}{d\Delta\rho/d\phi t}\right)_{\phi t_{max}}$
Al(1)	10.19	8.15	8.83	Si	2	0.15	2×10^{-4}	2×10^{-4}
Ni	9.52	7.62	8.25	Co + Fe	160			
Cu(1)	9.80	7.84	8.49	Ni + Zn	34	2.5	8×10^{-3}	2×10^{-3}
Pd	12.07	9.65	10.46	Ag	33			
Ag(1)	10.07	8.06	8.73	Cd	1200	44.0	0.12	0.26
Pt(1)	10.07	8.06	8.73	Au + Hg	3			
Au	11.83	9.46	10.25	Hg	1500	62.0	0.12	0.26
Fe	9.52	7.62	8.25	Mn + Co	<1			
Sn	11.83	9.46	10.25	Sb	<1			

tions $\Delta\rho_{max}^{FA}$ have been calculated (when interesting) from the specific FA resistivities as quoted, e.g., in Ref. 29. Again, for the end of the irradiation Table II shows which fractions of the experimental $\Delta\rho(d\Delta\rho/d\phi t)$ are due to the FA ($\Delta\rho^{FA}$) only and so cannot be due to the Frenkel defects. Matthiessen's rule was always considered as fulfilled. Due to Table II, corrections for transmutations are only essential for Ag and Au, and so a computer correction was performed in these cases and the corrected data are also shown in Figs. 8 and 10 (here $\Delta\rho_{exp}$ is replaced by $\Delta\rho_{exp} - \Delta\rho^{FA}$).

The characteristic results of the computer fits to the differentiated dose curves are collected in Table III. The values ρ_F are the specific FD resistivities taken from the literature. For all samples one best fit to Eq. (3) was selected and the range of $\Delta\rho$ used for the fit as well as the normalized coefficients are given. Usually this best fit is a cubic fit as in Eq. (3), with the exception of Al, where $C>0$ was obtained only for the quadratic ($D=0$), and not for the cubic fit. The quality of these best fits can be seen from the plots $(d\Delta\rho/d\phi t)_{exp} - (d\Delta\rho/d\phi t)_{fit}$ in Figs. 4–10. The extrapolated saturation resistivities $\Delta\rho_s$ (defined by $d\Delta\rho/d\phi t=0$) are given for linear fits to Eq. (1) as well as for quadratic and cubic fits to Eq. (3). Here the figures in parentheses are the limits of $\Delta\rho$ used for these fits and a dash indicates that a given fit does not go through zero [i.e., always $(d\Delta\rho/d\phi t)_{fit}>0$]. For the recombination volumes v_0, the results from Eq. (5) are generally the best ones since they consider also subthreshold recombination. These data v_0 have been obtained from the best fits as listed in Table III, and a dash indicates that v_0 was imaginary because $c<0$. For comparison we have also calculated v_0 from Eq. (8) using the extrapolated saturation resistivities $\Delta\rho_s$ from the cubic fits of Table III.

The cubic test means the left-hand side of Eq. (7), which should be close to -1. Finally, the relative contribution x of subthreshold effects to the total radiation annealing has been obtained from the right-hand part of Eq. (9) and using again the best-fit coefficients.

C. Discussions of dose curves

Generally speaking, the agreement between the various experiments and the cubic computer fits is fairly good as seen in Figs. 4–10. However, in Table III each value of the left-hand side of Eq. (7) (the cubic test) is far from -1, as would be necessary if Eq. (2) were strictly fulfilled. Further, there are many cases where the condition $D<0$ is not obeyed [see Eq. (4)], but the most striking violation of this theory occurs for those four metals where even C has the wrong (i.e., negative) sign [cf. Eq. (5)]. Thus, there is rather strong disagreement between the present theory and our high-dose experimental results. A first reason for this discrepancy is certainly that the theory is an electron-irradiation theory which neglects cascade effects occuring in fast-neutron irradiations. A second reason will be discussed below.

From Table III the convex curvature of the differentiated dose curve (i.e., $C<0$) is common to Ni, Pd, Pt, and also to Fe. This negative curvature can also be seen directly in Figs. 5, 7, and 9, and Ref. 26. The iron dose curve reported by Horak and Blewitt[15] seems to show it, too, but the larger data scatter and much smaller irradiation dose (about 20% as compared with ours[26]) did not allow them to recognize this convex curvature at that time. This behavior cannot be explained within the framework of usual defect-production theory, where the overlap of recombination vol-

TABLE III. Results of the computer fits to the dose curves. The values ρ_F (defined by $\Delta\rho = \rho_F c$) are taken from the literature. The fit coefficients are only given for characteristic "best fits" to Eq. (3); for Ag(1) and Au this is both without and with corrections for transmutations (FA) performed before making the fits. The $\Delta\rho_s$ are the extrapolated saturation resistivities [$d\Delta\rho/d\phi t = 0$ in Eq. (1) or Eq. (3)] and the values in parentheses are the fit limits used. The recombination volumes v_0 have been obtained from Eq. (5) and using the "best-fit" coefficients; these values v_0 should be more realistic than those obtained from Eq. (8) with the "cubic-fit" extrapolations $\Delta\rho_s$. The column "cubic test" means the left-hand side of Eq. (7) which should normally be close to −1. The subthreshold contribution x to radiation annealing is obtained from the right-hand part of Eq. (9) with the "best-fit" coefficients.

Sample	ρ_F $\frac{n\Omega\,cm}{ppm}$ Reference	Fit limits (nΩ cm)	Best fit to Eq. (3) B/A $\left(\frac{10^{-3}}{n\Omega\,cm}\right)$	C/A $\left(\frac{10^{-3}}{n\Omega\,cm}\right)^2$	D/A $\left(\frac{10^{-3}}{n\Omega\,cm}\right)^3$	Extrapolated $\Delta\rho_s$ (nΩ cm) Linear fit	Quad. fit	Cubic fit	v_0 (at. vol) From Eq. (5)	From Eq. (8)	Cubic test Eq. (7)	Subthreshold Eq. (9)
Al(1)	0.40	50–800	−1.200	+0.143	···	885 (50–400)	927 (50–800)	955 (50–866)	151	418	···	+0.370
Al(2)	Refs. 22, 33, 34	50–800	−1.197	+0.130	···	879 (20–400)	922 (50–800)	944 (20–850)	144	424	···	+0.398
Al(3)		20–800	−1.228	+0.167	···	869 (100–400)	913 (20–800)	940 (20–850)	164	426	···	+0.334
Al(4)		20–800	−1.192	+0.112	···	870 (20–400)	917 (20–800)	955 (20–880)	134	419	···	+0.439
Ni	0.64 Refs. 14, 15	50–1000	−0.545	−0.221	−0.069	1562 (100–400)	1347 (50–1000)	1390 (50–1000)	···	460	$C<0$	$C<0$
Cu(1)	0.22	0–320	−3.194	+1.600	+1.044	353 (20–200)	422 (0–320)	435 (0–320)	278	506	52.0	+0.208
Cu(2)	Refs. 33, 36	0–320	−3.267	+2.179	−0.036	354 (20–200)	421 (0–300)	438 (0–320)	325	502	−1.12	+0.096
Pd	0.9 Ref. 37	200–1100	−0.602	−0.242	+0.120	1368 (200–1000)	1363 (200–1100)	1421 (200–1100)	···	633	$C<0$	$C<0$
Ag(1)	0.25	0–360	−3.133	+3.923	−2.579	414 (30–200)	··· (0–360)	580 (0–360)	495	431	−33.2	−0.264
Ag(2)	Refs. 14, 15	0–360	−2.937	+3.245	−1.650	420 (30–200)	··· (0–360)	633 (0–360)	450	395	−28.2	−0.227
Ag(3)		0–360	−3.123	+3.669	−1.950	409 (30–200)	··· (0–360)	630 (0–360)	479	397	−27.7	−0.227
Ag(1) FA corr.		0–320	−3.702	+5.589	−5.666	355 (28–184)	··· (0–320)	425 (0–320)	591	588	−42.9	−0.227
Pt(1)	0.70	500–1160	−0.313	−0.120	+0.025	2317 (500–1000)	2094 (500–1160)	1954 (500–1160)	···	358	$C<0$	$C<0$
Pt(2)	Refs. 1, 33	0–1260	−0.397	−0.011	−0.040	2201 (0–1260)	1970 (0–1260)	1819 (0–1260)	···	385	$C<0$	$C<0$
Au	0.33	50–500	−1.295	+0.911	−0.334	957 (50–300)	··· (50–500)	1478 (50–500)	315	223	−38.4	−0.474
Au FA corr.	Ref. 1	50–450	−1.779	+0.980	−0.073	663 (50–280)	··· (50–450)	1000 (50–450)	327	250	−7.4	−0.113
Fe	1.9 Refs. 39, 40	0–4350	−0.081	−0.025	+0.002	8050 (500–1500)	5819 (0–4350)	6425 (0–4350)	···	296	$C<0$	$C<0$
Sn	1.1 Ref. 41	20–490	−2.340	+1.773	−1.566	536 (20–490)	558 (20–490)	544 (20–490)	1465	202	−66.4	−0.138

umes would always lead to a decrease of the average recombination volume per FD, and so, to a positive (i.e., concave) curvature.[2-5,21] Since Fe and Ni are ferromagnetic (and Pd is nearly so), it might be possible that this peculiar behavior is somehow connected with, or at least favored by, the ferromagnetic nature of these metals (e.g., caused by magnetoresistance or Bloch-wall effects). Nevertheless, such an interpretation would still be incomplete because the metals Pt and Pd are nonmagnetic.

Quite generally, the physical origin of this convex curvature should be a concentration dependence of the specific FD resistivity ρ_F (as usually ρ_F is the specific resistivity of a unit concentration $c=1$ of FD). There is theoretical[21,23,30] and experimental[22] evidence that the specific resistivity of a given concentration of isolated defects should usually decrease when the defects agglomerate. Such an effect might already occur within a single-displacement cascade, which would be dose independent and not detectable in our measurements. However, if strong FD clustering occurs, as expected, during high-dose irradiation due to multiple overlap of cascades, this effect would be dose dependent. A decrease of ρ_F with dose would, indeed, impose a tendency towards convex curvature on all differential dose curves (Figs. 3, 5–10) because both axes are proportional to $\Delta\rho=\rho_F c$. If $dc(c)/d\phi t$ were plotted instead of $d\Delta\rho(\Delta\rho)/d\phi t$, the result could be concave again. As a conclusion, we expect a convex contribution to be present in the differentiated dose curves $d\Delta\rho(\Delta\rho)/d\phi t$ of all metals, but for some reasons this contribution is larger than the usual concave contribution in Fe, Ni, Pd, and Pt, and not in the other metals investigated so far.

Recently, this effect of convex curvature has been confirmed in a new high-dose reactor-irradiation experiment at 4.6 K in Munich,[31] where high-purity Fe and Ni samples were irradiated together with a conventional Fe sample (as in this paper) in a constant magnetic field of 1 KG. This effect has also been observed during reactor irradiation of conventional Fe at 20 K by the group in Paris,[32] but it is obviously absent in electron- or fission-fragment irradiations of Fe at 20 K (all without external field).[32] So the effect is certainly real and intrinsic and seems to depend on the type of radiation damage produced in Fe or Ni; i.e., the differentiated dose curves seem to be normal when either single defects or extremely dense defect clusters are produced, and anomalous when the clusters (cascades) are intermediate and not as dense. A possible systematic change of the reactor neutron spectrum with time very probably can not explain this anomalous effect, e.g., since Al or Cu samples irradiated simultaneously always behaved quite normally.

1. Aluminum

The four Al wire samples were used for the determination of the neutron-flux gradient in both

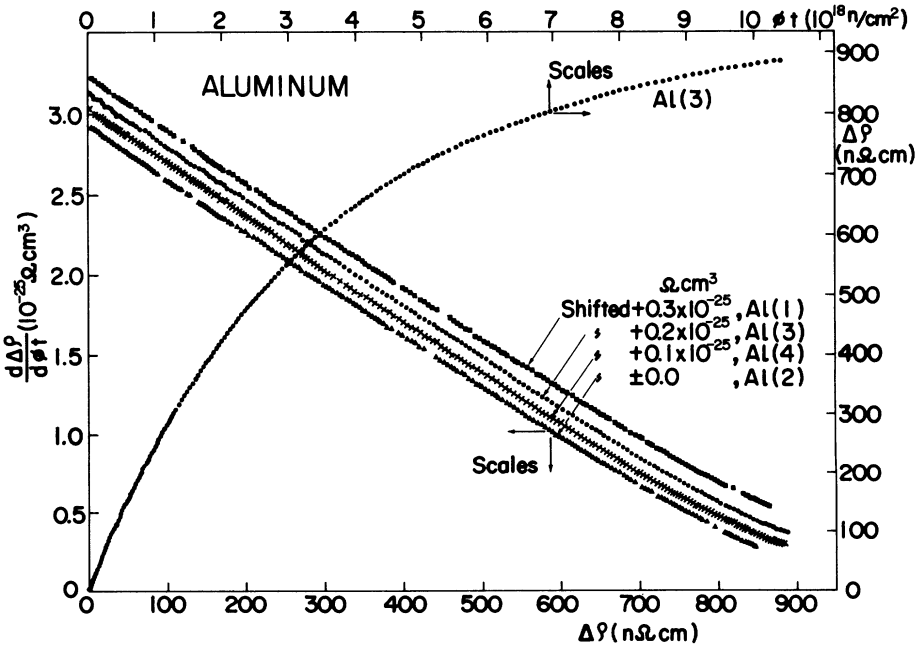

FIG. 3. Dose-curve results for Al. Only one typical curve of $\Delta\rho$ vs ϕt is shown [Al(3), right and top scales], but the differentiated curves $d\Delta\rho/d\phi t$ are shown for all samples. Transmutation corrections have not been performed.

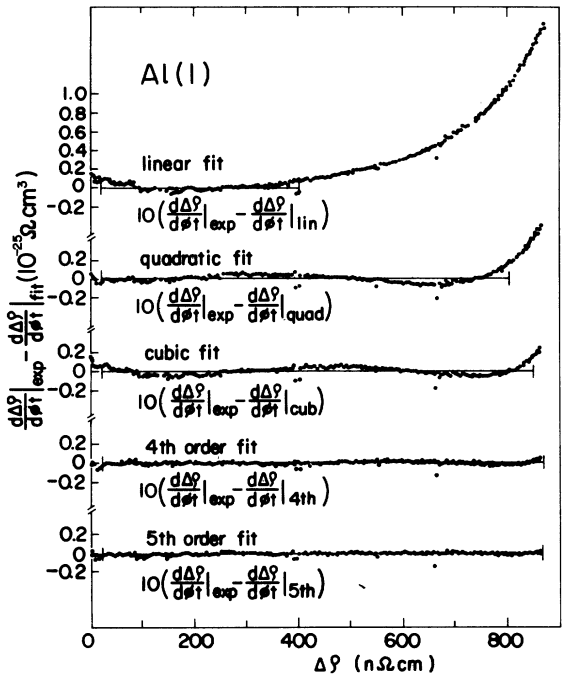

FIG. 4. Comparison of various computer fits $(d\Delta\rho/d\phi t)_{fit}$ to the experimental curves $d\Delta\rho/d\phi t = (d\Delta\rho/d\phi t)_{exp}$ for Al(1). The ranges of $\Delta\rho$ used for the fits are indicated by the horizontal bars, and the fits to Eq. (3) proceed from first order ($C=D=0$) to fifth order (new terms $E\Delta\rho^4+F\Delta\rho^5$ added). For the quadratic fit, the coefficients are given in Table III. Note the enlarged vertical scale.

sample holders and for a check of the experimental reproducibility. The highest achieved value of $\Delta\rho_{max}$ [Al(3)] corresponds to about 93% of the extrapolated $\Delta\rho_s$ (cubic fit), and the damage production rate $d\Delta\rho/d\phi t$ is already very close to zero, as shown in Fig. 3.

The differences in the local neutron flux (Table I) should not influence the extrapolated $\Delta\rho_s$.[25] From Table III this is certainly the case within ±8 nΩ cm. The differentiated dose curves are perfectly linear in a region of $\Delta\rho$ up to about 350 nΩ cm, and it was verified from measurements of the low-field Hall coefficient R_0 that this is just the same region of $\Delta\rho$ where dose-dependent FD clustering is still insignificant.[6]

A series of computer fits of the experimental data has been shown in Fig. 4; the fits to Eq. (3) proceed from first order ($C=D=0$) to fifth order (new terms $E\Delta\rho^4+F\Delta\rho^5$ added). As is easily seen, a fifth-order fit is virtually perfect; however, no theory is available for that. A cubic fit gave a negative value of C and so the quadratic fit is listed in Table III. As seen in Table III, we took $\rho_F = 0.40$ nΩ cm/ppm[22,33,34] for Al. The recombination volume v_0 is much smaller when subthreshold effects are included in its calculation [Table III, Eq. (5)] than otherwise [Table III, Eq. (8)], as also discussed in Ref. 25. The fraction x of subthreshold effects is slightly smaller than in Ref. 25. During low-temperature electron irradiation of Al, the concave curvature was much more pronounced than in our case (see Ref. 12).

2. Nickel

The resistivity increment $\Delta\rho_{max} = 1065.9$ nΩ cm corresponds to 77% of the extrapolated $\Delta\rho_s$ (cubic fit). The strong initial tail in the damage rate has been interpreted to result from long-range replacement collisions.[14] It is also possible to interpret this tail by magnetoresistance effects in the ferromagnetic Ni.[31] Such an initial tail was completely absent in Al (Fig. 3), but is known to be common to bcc metals from preliminary neutron-irradiation experiment by Dönitz *et al.*[35] The outstanding result is a negative curvature of the differentiated dose curve (Fig. 5), which has already been discussed.

3. Copper

Two samples were irradiated for the determination of the flux gradient in sample holder 1. The resistivity increment $\Delta\rho_{max} = 321.4$ nΩ cm corresponds to 74% of the extrapolated $\Delta\rho_s$ [cubic fit, Cu(1)]. The third-order computer fit in Fig. 6 reproduces the data surprisingly well. In Table III the fit coefficients and fit results have quite reasonable values, especially for Cu(2). We took $\rho_F = 0.22$ nΩ cm/ppm.[33,36] In contrast to the situation of Al, the differentiated dose curve of Cu as measured during electron irradiation[12] is almost linear and extrapolates up to about double the value of $\Delta\rho_s$, as in our case (or after fission irradiation[10]). This behavior probably has to do with the rather compact form of the cascades in neutron-irradiated Cu.[13]

4. Palladium

The resistivity increment $\Delta\rho_{max} = 1096.7$ nΩ cm corresponds to 77% of the extrapolated $\Delta\rho_s$ (cubic fit). The negative curvature ($C<0$) has already been discussed above. For ρ_F value in Table III, we took 0.9 nΩ cm/ppm after Jimenez *et al.*[37]

5. Silver

Three Ag wires were irradiated; two of them served for determing the flux gradient in the sample holder 2. This second run was up to $\Delta\rho_{max} = 408.1$ nΩ cm corresponding to about 65% of the extrapolated $\Delta\rho_s$ [cubic fit, Ag (2)]. The influence

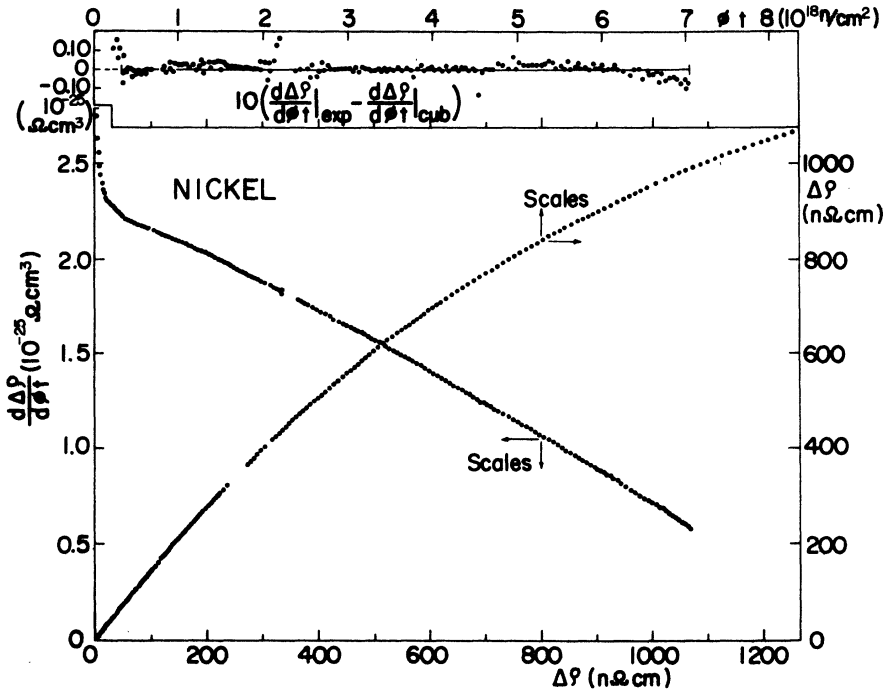

FIG. 5. Dose-curve results for Ni. Plot of the integral curve $\Delta\rho$ vs ϕt (right and top scales) and of the differentiated curve $d\Delta\rho/d\phi t$ vs $\Delta\rho$. The top diagram shows the difference between the experimental $d\Delta\rho/d\phi t$ and a computer fit to Eq. (3) on an enlarged vertical scale, compare Fig. 4 (fit coefficients in Table III). Transmutation corrections have not been performed.

of irradiation-induced transmutations on the production rate was large (see Table II). The corrected curve [Ag (1)] is also shown in Fig. 7. The fit coefficients always have the right sign, but the last two columns in Table III show unreasonable values (especially $x<0$). All pairs of values v_0 are unsystematic, too.

6. Platinum

Two Pt samples were irradiated in different runs. The data fluctuation of Pt (1) was very large in the first half of the irradiation, and rather normal in the second half. For Pt (2) the data fluctuation was always very large (a similar behavior of

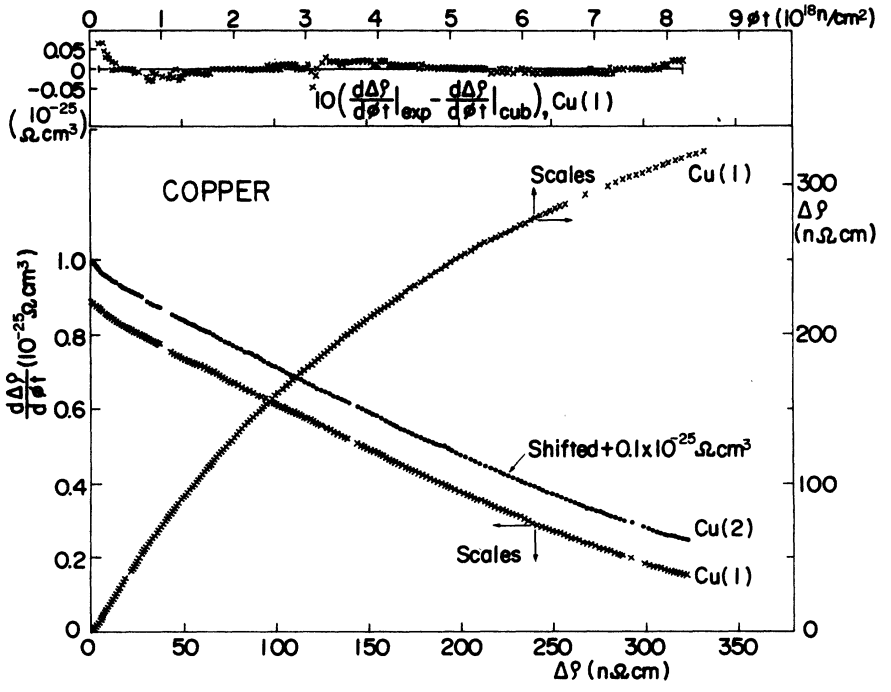

FIG. 6. Dose-curve results for Cu. For the presentation of the data, see caption of Fig. 5.

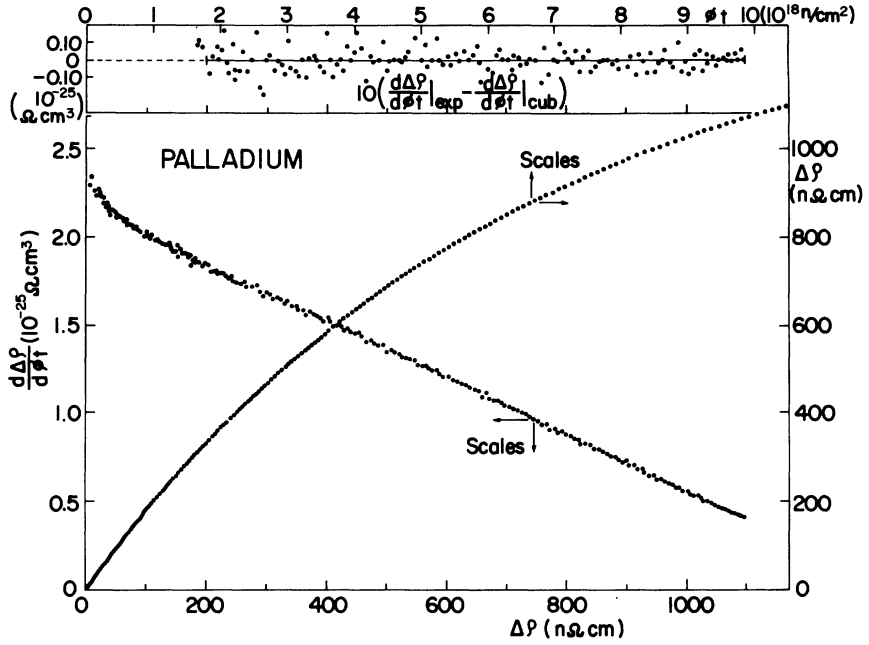

FIG. 7. Dose-curve results for Pd. For the presentation of the data, see caption of Fig. 5.

Pt was also observed in Ref. 15). Whatever the reason of this scatter may be, both production rate curves in Fig. 9 show the negative curvature in the high $\Delta\rho$ region, and consequently, $C<0$ in Table III as already discussed above. Similar to the situation for Cu, the differentiated dose curve of Pt behaves quite normally (rather linearly) during electron irradiation[12] and extrapolates to about double the value of $\Delta\rho_s$ as in our case. The resistivity increment $\Delta\rho_{max} = 1265.1$ nΩ cm corresponds to 70% of the extrapolated $\Delta\rho_s$ [cubic fit, Pt (2)].

7. *Gold*

Gold is a very special candidate in our experiments since it is known from other work[38] that free migration of the interstitials already occurs

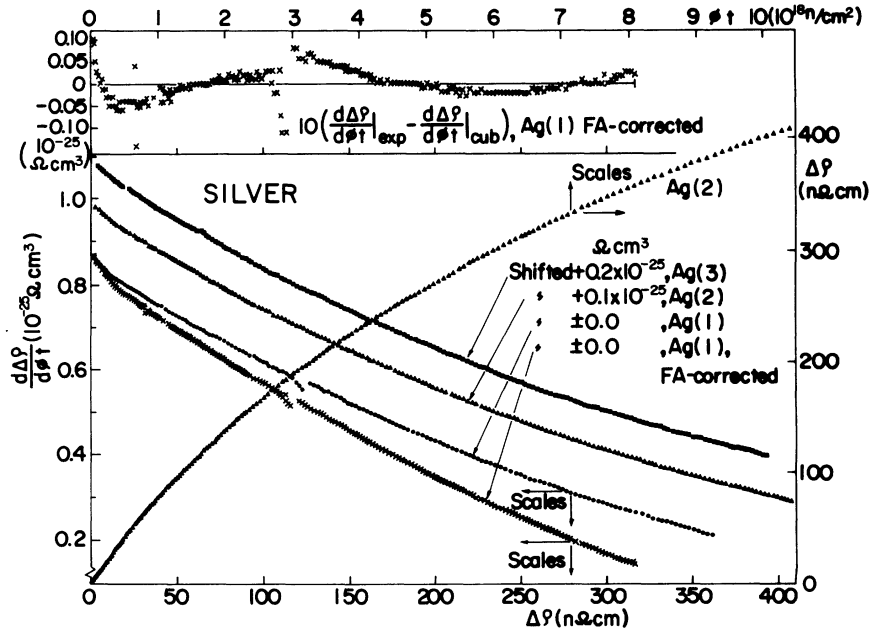

FIG. 8. Dose-curve results for Ag. For the presentation of the data, see caption of Fig. 5. Transmutation corrections have been performed only on the curves labeled "FA-corrected."

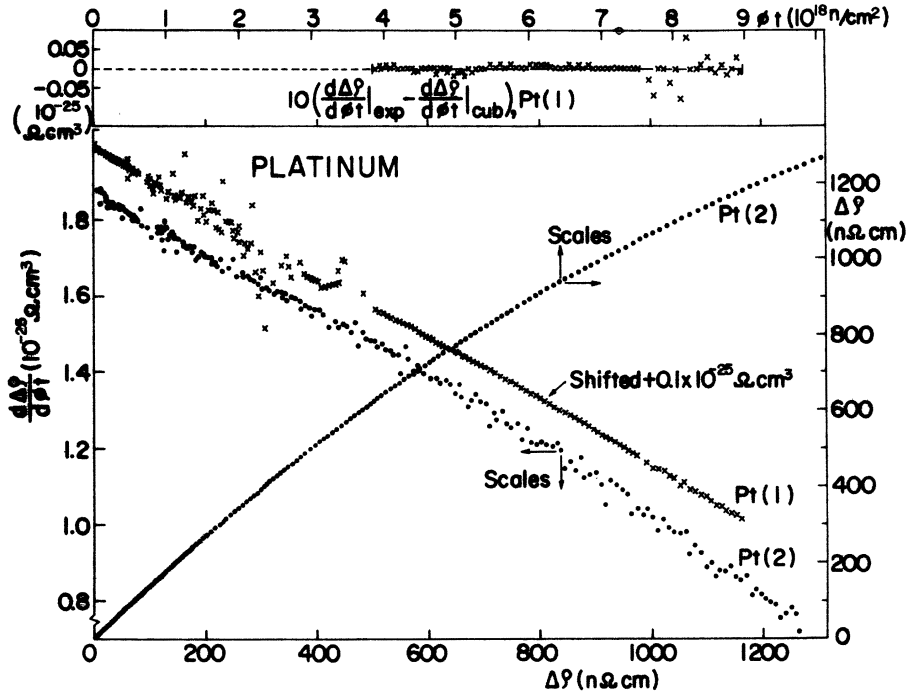

FIG. 9. Dose-curve results for Pt. For the presentation of the data, see caption of Fig. 5.

below 4 K in this metal. Thus it is clear that our theoretical formalism of Sec. III A cannot be applied in this case. The resistivity increment $\Delta\rho_{max}$ = 498.9 nΩ cm corresponds to only 34% of the extrapolated $\Delta\rho_s$ (cubic fit). As in the case of Ag, the influence of irradiation-induced transmutations on the differentiated dose curves is very large and is also shown in Fig. 10.

Iron and tin (Table III) are non-fcc metals and have been discussed elsewhere.[26,27] As to the ρ_F

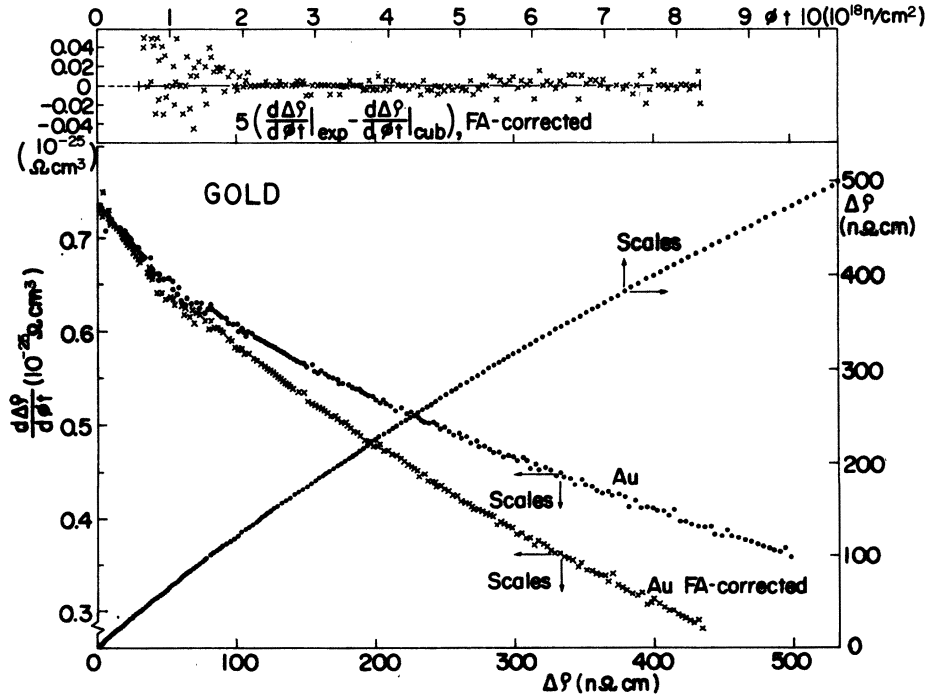

FIG. 10. Dose-curve results for Au. For the presentation of the data, see caption of Fig. 5. Transmutation corrections have been performed on the curves labeled "FA-corrected."

value, we took 1.9 nΩ cm/ppm,[39,40] and 1.1 nΩ cm/ppm,[41] for Fe and Sn, respectively. The negative curvature ($C<0$) in the differentiated dose curve of iron has also been discussed above.

D. Isochronal recovery

After the end of the two high-dose neutron irradiations at 4.6 K, isochronal recovery was performed up to temperatures of about 400 and 500 K, respectively. The data for this treatment were: first annealing step up to 20 K, temperature difference between two neighboring steps $\Delta T \approx 0.06T$, number of steps about 50, holding time for each annealing treatment 10 min. After each step the resistivity was measured at 4.6 K. Due to experimental accidents in one annealing treatment the data points between 32 and 43 K for Al, Pd, Ag, Pt, and Au were lost; for Cu and Ni, which were irradiated in the other run, annealing data exist only above 75 K.

In the following the annealing results will be listed. They will be compared with the results of previous experiments after reactor-neutron or fast-neutron irradiation at liquid-helium tempera-

TABLE IV. List of annealing results, compared with the results of previous experiments after reactor-neutron or fast-neutron irradiation at liquid-helium temperature.

		Stage I		Stage III	
Ref.	$\Delta\rho_{max}$ (nΩ cm)	Peak temp. (K)	Recovery (%)	Peak temp. (K)	Recovery (%)
		(a) Aluminum			
20	6.1	34	45	190, 240	30
45	118.8	39	44	190,[a] 220	33
43	382.3	35	40	210	37
42	593.0	35	35	195	40
Ours	881.6	34–37	25	190	50
		(b) Nickel			
42	5.4	54	37	350	17
43	363.9	56	33	···	···
42	587.7	53	31	~350	~20
Ours	1065.4	···	26	320	20
		(c) Copper			
20	2.0	38	34	225, 300	39
46	2.9	35–40	>30	225, 310	~25
43	116.2	38	31	225	>34
42	192.7	38	26	230, 275	35
Ours	321.4	···	<24	240	39
		(d) Silver			
20	2.0	28	28	210, 285	25
43	87.9	28	15	210	~39
42	201.3	28	15	220	43
Ours	408.1	26	7	215	43
		(e) Platinum			
42	4.9	Complex	37		
43	264.6	~20	34		
42	551.9	21	33		
Ours	1265.1	~20	25		
		(f) Gold			
20	1.7			235, 330	53
46	2.6			230, 330	~55
42	39.1			240, 290	51
43	102.7			~230,[a] 275	~50
42	216.5			~230,[a] 260	53
Ours	498.9			~230,[a] 255	54

[a]Shoulder.

ture. These will mainly be results of one of the many irradiations by Burger *et al.*[20,42] i.e., an irradiation of Al, Ni, Cu, Ag, Pt, and Au with rather low dose (3.6×10^{16} reactor neutrons/cm^2) and Horak and Blewitt,[43] who irradiated Al, Ni, Cu, Ag, Pt, and Au with 2.0×10^{18} fast neutrons/cm^2. For individual elements, results of other groups will be compared, too. Our aim is to demonstrate the changes in height and temperature of the recovery stages due to the large-defect concentrations generated in the present irradiation. Our aim in this work is not to discuss extensively the physical reasons of the experimentally observed trends in terms of models of interstitial and vacancy migration.

In Figs. 11–17, the recovery and the differential recovery as a function of annealing temperature are shown for the metals Al, Ni, Cu, Pd, Ag, Pt, and Au. The left ordinate is the percent recovery; the right ordinate is the temperature derivative of the resistivity recovery [percent recovery/log$T$(K)]; both are plotted as functions of the isochronal annealing temperature. Tables IV(a)–IV(f) give characteristic values for stages I and III of the various elements.

In the following, we list the general trends in the dose dependence of the annealing behavior of the fcc metals. Part of these trends are long well known (see, e.g., Ref. 7). Our irradiations permit us to study these trends up to neutron doses which are about a factor of 5 higher than those used by Horak and Blewitt[43] and more than a factor of 2 higher than those which Burger has used in one of his irradiations.[42]

(i) Stage I shows no shift in temperature with increasing dose. This indicates first-order kinetics (cf. Ref. 43) implying that in the displacement cascades created by the fast-neutron collisions a quasicorrelated recovery of migrating interstitials with neighboring vacancies takes place.

(ii) Stage I decreases with increasing dose. This indicates that with increasing defect density an increasing fraction of the interstitials cluster together during their migration (that is, already during irradiation) being thus lost for annihilation with vacancies in stage I.

(iii) Stage II is rather complex. No marked differences can be found when varying the irradiation dose by nearly three orders of magnitude.

(iv) Stage III consists of two peaks after low-dose irradiation. The high-temperature peak shifts with increasing dose to lower temperatures, merging at high dose together with the low-temperature peak.[7,44] The low-temperature peak has been suggested[44] to be due to the correlated recombination of migrating vacancies with immobile interstitials inside their native displacement cascades, whereas the high-temperature peak should be due to the uncorrelated recombination of the vacancies at sinks outside the zone. It is interesting to note

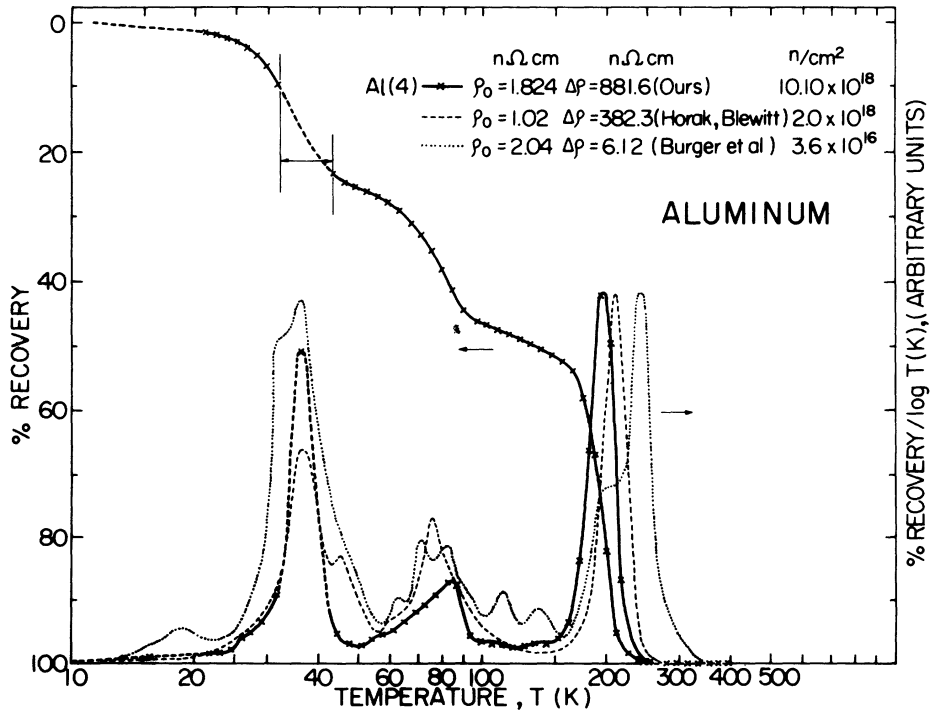

FIG. 11. Percent recovery and differential recovery vs logarithm of absolute temperature for Al.

that after extremely high-dose irradiation, the correlated recombination constitutes the total stage III, having gained in intensity at the cost of the uncorrelated recombination.

(v) The height of stage III increases with increasing dose. This must be a consequence of the decrease of stage I, and implies that with increasing dose an increasing fraction of interstitials by clustering has escaped recombination in stage I.

1. Aluminum

Stage I (defined as reaching up to 50 K) follows the general trends. It might be interesting that even at a defect concentration corresponding to our value of more than 90% of defect saturation, there is no significant shift of the stage to lower temperatures. Stage III begins at 150 K and ends at 250 K, also following the general trends, consisting at low doses of two subpeaks at 190 and 240 K, and merging at our extremely high dose to only one peak at about 190 K.

For comparison, recovery peaks observed by Burger *et al.*,[20] Dimitrov *et al.*,[45] Horak and Blewitt,[43] and by Burger[42] are also listed in Table IV(a). It is remarkable that even after a dose as high as in this work there is complete annealing after stage III at 250 K. This means that even at these extreme conditions no defect clusters remain after stage III. The conclusion from this finding may be the following: vacancies migrating in stage III highly prefer interstitials as reaction partner to any other type of sinks. Thus, even if the defect density is very high, the vacancies do not tend to cluster together during their migration or to annihilate at other sinks than interstitials.

2. Nickel

For Ni the data is above 80 K, and thus the complete stage I (definition, up to 65 K) has been lost; therefore, no statement about its temperature can be made. Its height follows the general trend. Stage II has a marked structure, the temperature of the peaks agreeing with lower-dose measurements. Stage III (above 260 K) can only be compared with Burger's data since it is incomplete in the work of Horak and Blewitt. It appears to follow the general trend.

3. Copper

As for Cu the data below 80 K was lost; therefore no conclusion on the temperature of stage I (up to 60 K) is possible. Its height follows the general tendency. The height of stage III defined here as between 170 and 320 K shows no clear dose dependence, implying that what appears as stage III might not be based on exactly the same processes after the different doses, making a comparison dubious. The two-peak structure

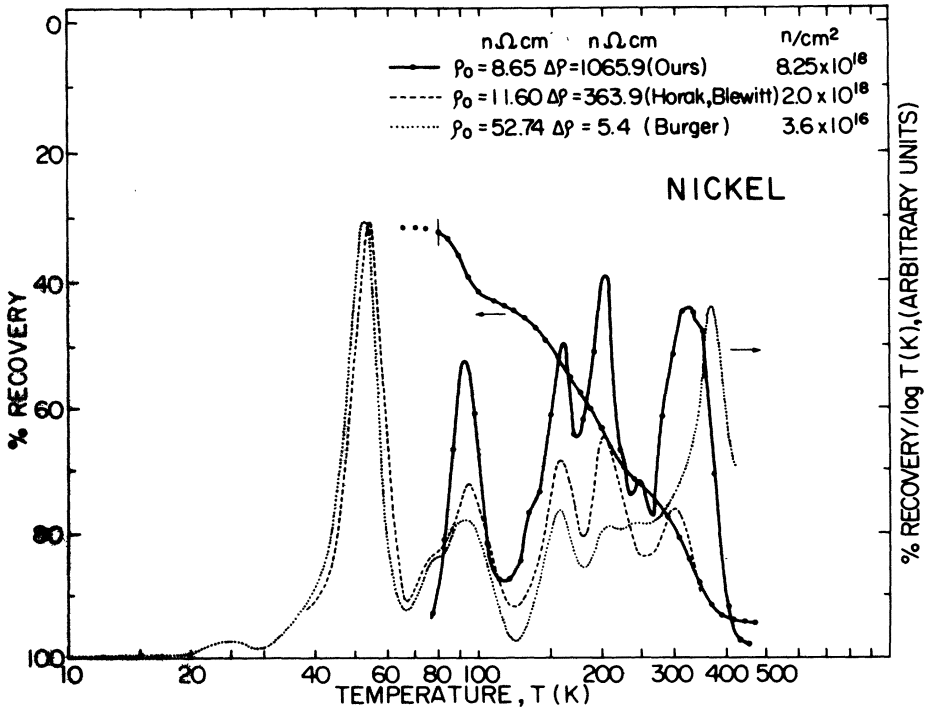

FIG. 12. Percent recovery and differential recovery vs logarithm of absolute temperature for Ni.

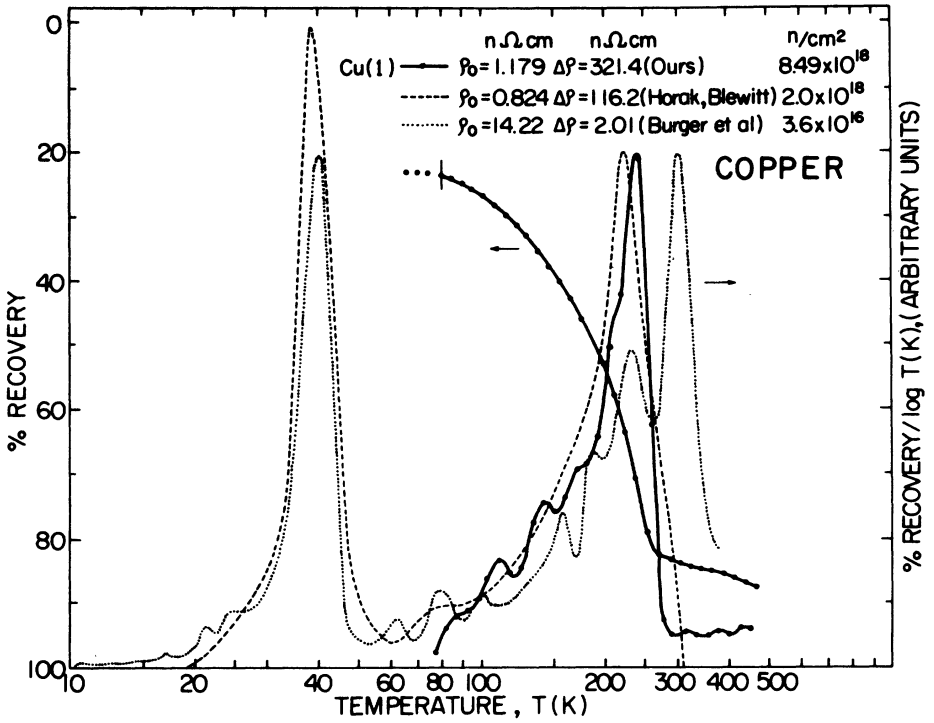

FIG. 13. Percent recovery and differential recovery vs logarithm of absolute temperature for Cu.

follows the general trend; thus we think the interpretation is that given above in (iv). Horak and Blewitt,[43] on the contrary, explain the high-temperature peak as a consequence of the damage from thermal neutrons due to (n,γ) processes present in Burger's[20] and Takamura's[46] reactor-neutron spectrum, but absent in the fission-neutron spectrum which Horak and Blewitt used. Our result

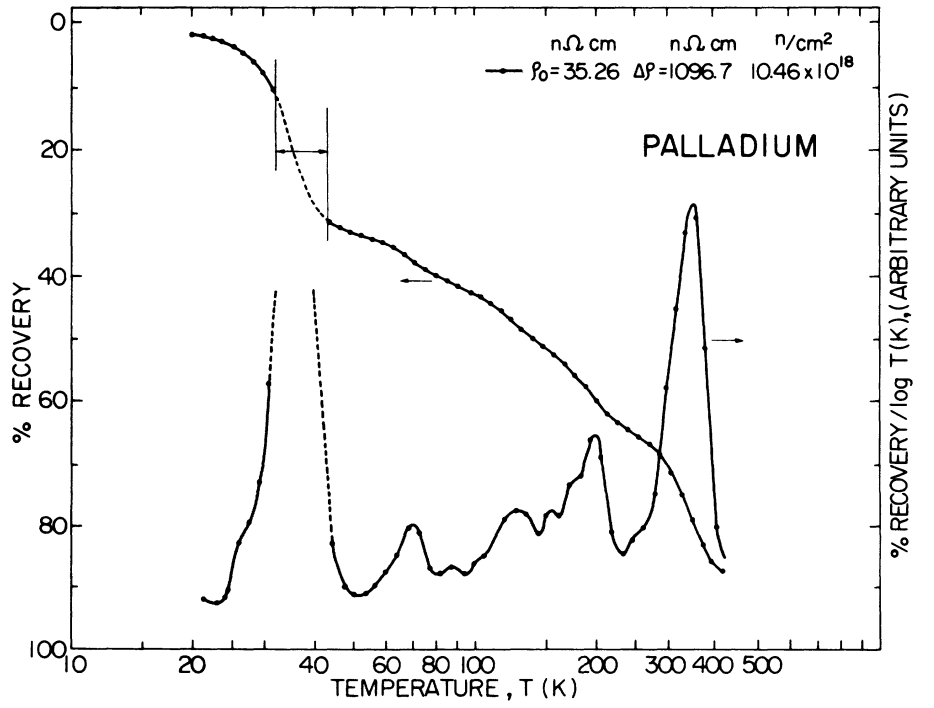

FIG. 14. Percent recovery and differential recovery vs logarithm of absolute temperature for Pd.

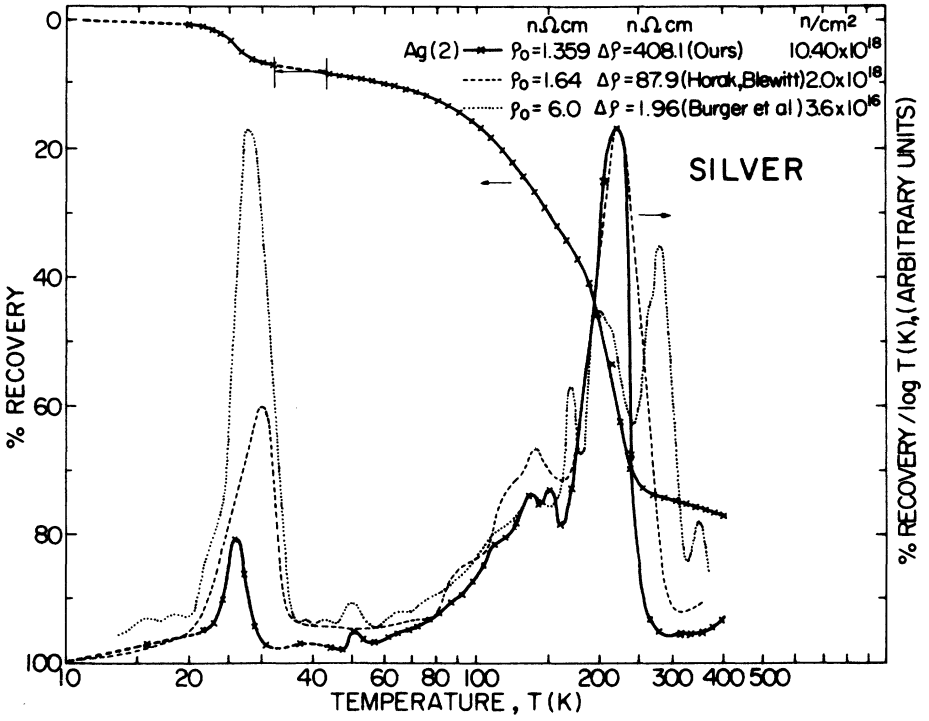

FIG. 15. Percent recovery and differential recovery vs logarithm of absolute temperature for Ag.

now shows that this explanation cannot be fully correct since we have also used a reactor-neutron spectrum, but did not find the 300-K peak (and we have calculated the influence of transmutations to be small, see Table II). Because of the unclearness of the detailed behavior of stage III in Cu, however, our conclusion also remains a hypothesis.

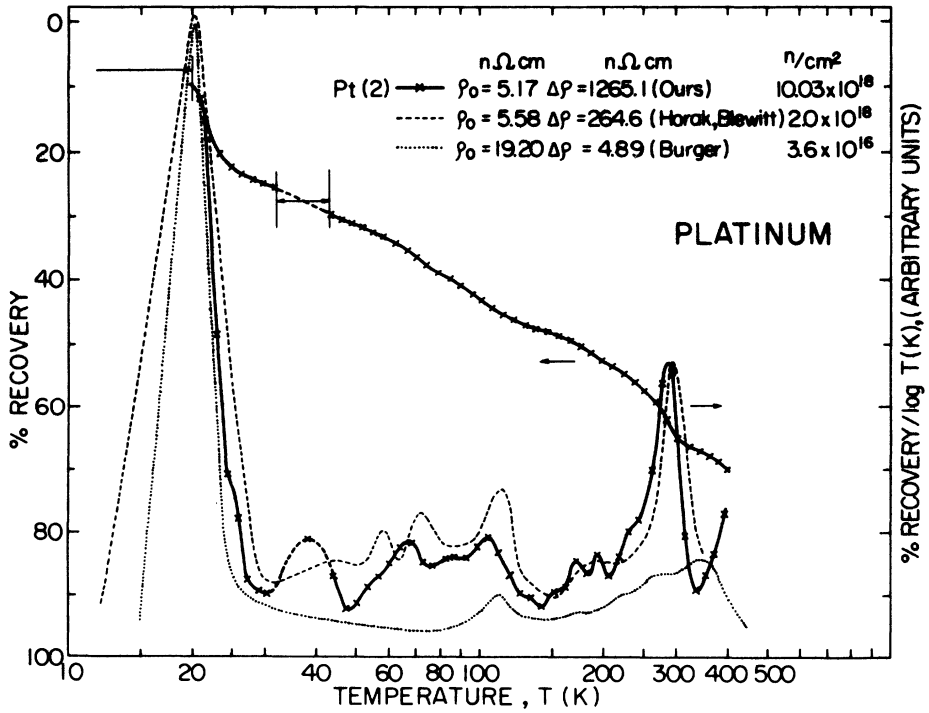

FIG. 16. Percent recovery and differential recovery vs logarithm of absolute temperature for Pt.

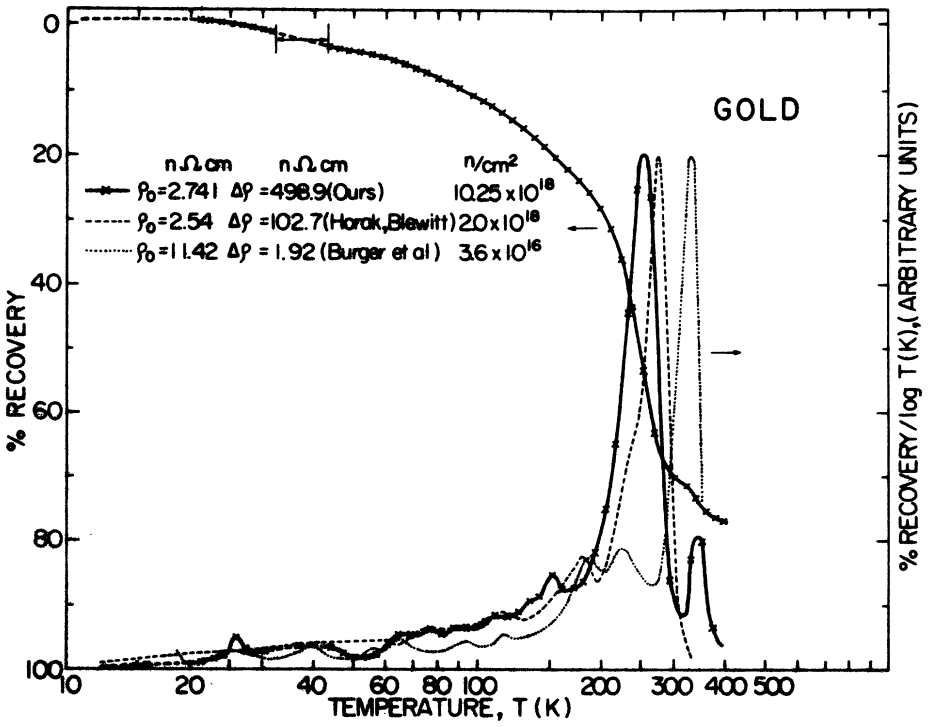

FIG. 17. Percent recovery and differential recovery vs logarithm of absolute temperature for Au.

4. *Palladium*

There is not sufficient other data available to compare with our present work.

5. *Silver*

The trends of stage I (ending at 40 K) and stage III (counted from 170 to 400 K) are as usual.

6. *Platinum*

The height of stage I (up to 30 K) decreases with increasing dose. No conclusion on the dose dependence of its temperature can be drawn from the present work. Since our annealing treatment ended at 400 K, we are not able to make comments about the annealing above 200 K. The identification of stage III in Pt to definite defect reactions is still controversial.

7. *Gold*

Gold does not possess a significant low-temperature annealing stage. It is known from other work[38] that interstitials are mobile already below 4 K in Au. Stage III between 170 and 400 K shows the general trend with two peaks merging together at high dose, but no clear dose dependence in its height. It is interesting that beside the main peak at 255 K there is another subpeak at about 340 K which has previously also been observed by Burger.[42]

IV. SUMMARY

The rate of resistivity increase as a function of irradiation-induced resistivity of fcc metals (Al, Ni, Cu, Pd, Ag, Pt, and Au) is generally nonlinear; computer analysis shows that most of the data are best fitted with an expression having up to third-order terms in $\Delta\rho$. In cases of aluminum, copper, silver, and gold the experimental curves have a positive deviation from a linear law (concave curvature); however, an anomalous negative deviation (convex curvature) is observed in nickel, palladium, and platinum as well as in iron, as reported previously.[26]

The apparent disagreement between our dose-curve results and the present theory is explained as being most probably caused by the neglect of cascade effects in this theory and by a decrease of the specific FD resistivity ρ_F due to the strong defect clustering in high-dose neutron irradiations.

The influence of irradiation-induced transmutations on the dose curves (FA corrections) are considered, but these are found to be essential only for silver and gold. Saturation values of the resistivity have been obtained as well as saturation defect concentrations and recombination volumes.

The isochronal recovery is compared with previous low-dose data (mainly by Burger *et al.*[20,42] and by Horak and Blewitt[43]). The height of stage I decreases, that of stage III increases with increasing dose for most of the metals. After high-

dose neutron irradiation (about 1×10^{19} fast neutrons/cm^2), correlated recovery in stage III becomes dominant in cases of aluminum, copper, silver, and gold.

ACKNOWLEDGMENTS

We are grateful to Professor H. Vonach and Professor W. Gläser for the kind support of this work and to the staffs of the liquid-helium irradiation facility and of the Research Reactor Munich (FRM) for their continuous help and cooperation. We thank Drs. C. E. Klabunde and R. R. Coltman of Oak Ridge National Laboratory for critically reading the manuscript and making valuable suggestions. One of the authors (M.N.) gratefully acknowledges Director Professor T. Shibata of Research Reactor Institute, Kyoto University for opportunity to carry out this research at FRM.

*Research supported by "Bundesministerium für Forschung und Technologie."

†Present address: Research Reactor Institute, Kyoto University, Kumatori-cho, Osaka 590-04, Japan.

[1]H. J. Wollenberger, in *Vacancies and Interstitials in Metals* (North-Holland, Amsterdam, 1970), pp. 215–253.

[2]G. Lück and R. Sizmann, Phys. Status Solidi 5, 683 (1964).

[3]G. Lück and R. Sizmann, Phys. Status Solidi 6, 263 (1964).

[4]M. Balarin and O. Hauser, Phys. Status Solidi 10, 475 (1965).

[5]K. Dettmann, G. Leibfried, and K. Schroeder, Phys. Status Solidi 22, 423 and 433 (1967).

[6]K. Böning, W. Mauer, K. Pfändner, and P. Rosner, Radiat. Eff. 29, 177 (1976).

[7]W. Schilling, G. Burger, K. Isebeck, and H. Wenzl, in Ref. 1, pp. 255–361.

[8]W. Schilling and K. Sonnenberg, J. Phys. F 3, 322 (1973).

[9]C. Weinberg, J. Dural, R. R. Conte, J. Leteurtre, G. Vogl, and K. Böning, Phys. Status Solidi A 1, K151 (1970).

[10](a) R. C. Birtcher, T. H. Blewitt, B. S. Brown, and T. L. Scott, Proceedings of the International Conference on Fundamental Aspects of Radiation Damage in Metals, Gatlinburg, Tenn., 1975 (unpublished); (b) Report No. CONF-751006-P1, 1976 (unpublished), p. 138.

[11]S. Klaumünzer, H. Neumüller, and G. Ischenko (unpublished).

[12]G. Duesing, W. Sassin, W. Schilling, and H. Hemmerich, Cryst. Lattice Deffects 1, 55 (1969).

[13]B. von Guerard and J. Peisl, in Ref. 10(a), p. 287.

[14]G. Burger, H. Meissner, and W. Schilling, Phys. Status Solidi 4, 281 (1964).

[15]J. A. Horak and T. H. Blewitt, Phys. Status Solidi 9, 721 (1972).

[16]*American Institute of Physics Handbook*, 3rd ed. (McGraw-Hill, New York, 1972), Chaps. 9-39.

[17]H. Meissner, W. Schilling, and H. Wenzl, Euronuclear 2, 277 (1965).

[18]W. Waschkowski, supplement to Report of Physik Dept., Techn. Univ., München, 1975 PTUM-FRM-115 (unpublished).

[19]K. Böning and H. Wenzl, supplement to Report of Physik Dept., Techn. Univ., München, 1967, PTUM-FRM-92 (unpublished).

[20]G. Burger, K. Isebeck, J. Völkl: W. Schilling, and H. Wenzl, Z. Angew. Phys. 22, 452 (1967).

[21]L. C. R. Alfred, Phys. Rev. 152, 693 (1966).

[22]P. Ehrhart and W. Schilling, Phys. Rev. B 8, 2604 (1973).

[23]J. W. Martin, J. Phys. F 2, 842 (1972).

[24]W. Köhler and W. Schilling, Nukleonik 7, 389 (1965).

[25]O. Dimitrov, C. Dimitrov, P. Rosner, and K. Böning, Radiat. Eff. 30, 135 (1976).

[26]M. Nakagawa, K. Böning, P. Rosner, and G. Vogl, Phys. Lett. A 56, 481 (1976). The annealing value 800 °C in a vacuum of 5×10^{-4} Torr should be corrected to 800 °C in a vacuum of 2×10^{-5} Torr. The scale of ϕt in Fig. 1 should be multiplied 1/1.30; e.g., ϕt_{max} in Tables I and II in this paper is correct.

[27]M. Nakagawa, K. Böning, W. Mansel, P. Rosner, and G. Vogl (unpublished).

[28]R. R. Coltman, C. E. Klabunde, and J. K. Redman, Phys. Rev. 156, 715 (1967).

[29]R. R. Coltman, C. E. Klabunde, D. L. McDonald, and J. K. Redman, J. Appl. Phys. 33, 3509 (1962).

[30]Mark T. Robinson, Atomic Energy Res. Establ. AERE-Report R7934 (unpublished).

[31]B. M. Pande, P. Rosner, K. Böning, H. E. Schaefer, A. Dunlop, and J. C. Jousset (unpublished).

[32]A. Dunlop, J. C. Jousset, and N. Lorenzelly (private communication).

[33]H. Wenzl, in Ref. 1, pp. 363–423.

[34]P. Ehrhart, H. G. Haubold, and W. Schilling, Adv. Solid State Phys. 14, 87 (1974).

[35]W. Dönitz, P. Rosner, W. Mansel, and K. Böning (unpublished).

[36]P. Ehrhart and U. Schlagheck, J. Phys. F 4, 1575 (1974).

[37]C. M. Jimenez, L. F. Lowe, E. A. Burke, and C. H. Sherman, Phys. Rev. 153, 735 (1967).

[38]P. Ehrhart and E. Segura, Proceedings of the International Conference on Fundamental Aspects of Radiation Damage in Metals, Gatlinburg, Tenn., 1975 (unpublished), R. C. Birtcher, W. Hertz, G. Fritsch, and J. E. Watson, *ibid.* p. 405 (unpublished).

[39]M. Biget, R. Rizk, P. Vajda, and A. Bessis, Solid State Commun. 16, 949 (1975).

[40]P. G. Lucasson and R. M. Walker, Phys. Rev. 127, 485 (1962).

[41]J. McIlwain, R. Gardiner, A. Sosin, and S. Myhra, Radiat. Eff. 24, 19 (1975).

[42]G. Burger, thesis (Technische Hochschule, München, Germany, 1965) (unpublished).

[43]J. A. Horak and T. H. Blewitt, J. Nucl. Mater. 49, 161 (1973–1974); errata, *ibid.* 50, 315 (1974).

[44]C. Frois and O. Dimitrov, C. R. Acad. Sci. (Paris) 258, 5647 (1964).

[45]C. Dimitrov, F. Moreau, and O. Dimitrov, J. Phys. F 5, 385 (1975).

[46]S. Takamura, H. Maeta, and S. Okuda, J. Phys. Soc. Jpn. 26, 1120 (1969).